The Fabrication of Bioresorbable Implants for Bone Defects Replacement Using Computer Tomogram and 3D Printing

P. G. Kuznetsov[1], S. I. Tverdokhlebov[1,a)], S. I. Goreninskii[1], E. N. Bolbasov[1], A. V. Popkov[2], D. E. Kulbakin[3], E. G. Grigoryev[3], N. V. Cherdyntseva[3], and E. L. Choinzonov[1,3]

[1] *Tomsk Polytechnic University, Tomsk 634050 Russia*
[2] *Russian Ilizarov Scientific Center for Restorative Traumatology and Orthopaedics, Kurgan 640014 Russia*
[3] *Cancer Research Institute, Tomsk National Research Medical Centre of the Russian Academy of Sciences, Tomsk, 634028 Russia*

[a)] Corresponding author: tverd@tpu.ru

Abstract. The present work demonstrates the possibility of production of personalized implants from bioresorbable polymers designed for replacement of bone defects. The stages of creating a personalized implant are described, which include the obtaining of 3D model from a computer tomogram, development of the model with respect to shape of bone fitment bore using Autodesk Meshmixer software, and 3D printing process from bioresorbable polymers. The results of bioresorbable polymer scaffolds implantation in pre-clinical tests on laboratory animals are shown. The biological properties of new bioresorbable polymers based on poly(lactic acid) were studied during their subcutaneous, intramuscular, bone and intraosseous implantation in laboratory animals. In all cases, there was a lack of a fibrous capsule formation around the bioresorbable polymer over time. Also, during the performed study, conclusions were made on osteogenesis intensity depending on the initial state of bone tissue.

INTRODUCTION

At the present stage of the development of the reconstructive and plastic surgery, the need for development and introduction of synthetic (composite) tissue-substitutive materials designed to reduce surgical trauma and complications while maintaining high efficiency is becoming increasingly evident [1, 2]. Biodegradable polymers such as poly(lactic acid) and poly(ε-caprolactone) became widely used in production of biomedical devices due do their biocompatibility and ability to resorb [3]. To increase the ability of such materials to substitute bone tissue, a number of modification methods were developed [4, 5].

There are a number of requirements to implants for bone defects replacement. The implant must fit the shape, volume, structure and consistency of the tissue and function of the organ that is restored. Mismatch of the geometry of osteoimplant and geometry of the resected fragment of facial skeleton entails limited mechanical functionality, a violation of facial mimics and articulation [6]. Simultaneous replacement of the defect requires the development of original medical personalized product that includes stages of diagnosis, visualization of the alleged defect based on use of computed tomography, computer simulation of the planned implant, manufacture of the model, supporting framework of the implant, modification of surface properties of the implant in accordance with individual characteristics of each clinical case. Such approach can be realized only with the use of 3D technologies, which are a world trend in creation of biocompatible materials for osteosubstitution.

Physics of Cancer: Interdisciplinary Problems and Clinical Applications
AIP Conf. Proc. 1882, 020040-1–020040-6; doi: 10.1063/1.5001619
Published by AIP Publishing. 978-0-7354-1562-1/$30.00

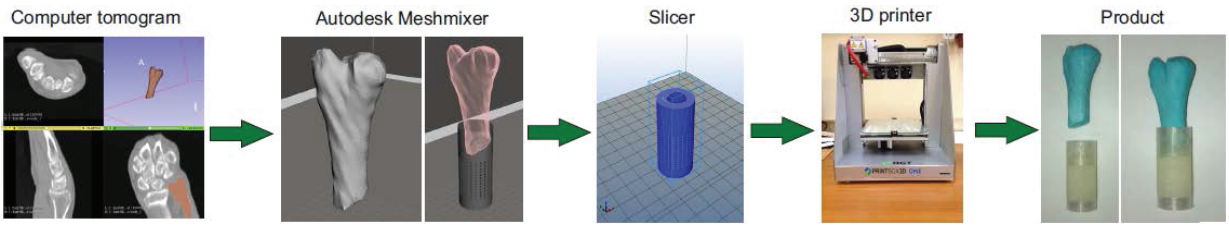

FIGURE 1. Stages of 3D implant fabrication

MATERIALS AND METHODS

Technology of Biodegradable 3D Implants Fabrication

The technology of bone structure modeling is based on complex processing of the obtained medical images and includes a number of stages. First of all, computer tomography is being conducted. Multispiral scanning in soft or bone tissue regime with slices thickness of not greater than 0.5 mm is taken as standard. The obtained models have DICOM format and are used at the next stage, virtual modeling. For that purpose, additional software is used to convert DICOM files into .stl files. In our case 3Dslicer software was used for multistep modeling: 1) cropping the "area of interest" of 3D-printing; 2) artefacts cutting; 3) selection of the densities range (not less than 150 Hounsfield units for bone tissue); 4) the smoothing and reduction of background noise. The listed manipulations result in the virtual model of the "area of interest" in .stl format. Then, the obtained model may be used for 3D printing or for production of the personalized implant with bone fitment bore. After 3D modeling, 3D model is being prepared for printing. Stl file is being loaded to slicer program that is used for preparation of the model for printing. 3D printing of the implant is conducted after all preparation steps. The stages of implant fabrication are presented in Fig. 1.

Investigation of Osteointegrative Properties of Poly(Lactic Acid)-Based Implants

To investigate the ability of bioresorbable poly(lactic acid)-based implants to integrate into bone tissue we used non-woven implants produced by previously reported method [7]. In vitro studies of bioresorbable poly(lactic acid)-based materials were presented earlier [8]. The osteointegrative properties of non-woven implants were tested on 48 male Wistar rats with mass of 180–200 g grown in E.D. Goldberg Scientific and research institute of pharmacology and regenerative medicine. The experiments were carried out according to the principles set out in EU prescriptions (86/609/EEC) and Helsinki declaration.

Three groups consisting of 16 animals were formed:

1. Animals with implanted biodegradable implant made of PURASORB PL-38 poly(lactic acid);
2. Animals with implanted composite implant made of PURASORB PL-38 poly(lactic acid) and mineral filler made of dihydrous dicalcium phosphate and produced by laser ablation method;
3. Animals with implanted composite implant made of PURASORB PL-38 poly(lactic acid) and mineral filler made of hydroxyapatite and produced by laser ablation method.

Implantation of Non-Woven Materials

Material implantation was performed under general mixed intramuscular anesthesia (anesthetics dose was calculated according to the animal's mass from the following proportions: 5–7 mg/kg of Zoletil and 4 mg/kg of Rometar). After the analysis of the anatomical and physiological features of the rats, two areas were selected for extramedullary implantation: calvarial (or parietal) and pelvic (or upper hip) bones.

Cranial bones access was achieved on midline via skin dissection and lateral traction of temporal muscles with parietal bone cortex using raspatory. Access to upper hip bones was obtained from the right and left sides in longitudinal direction. The length of skin incision was from 12 to 20 mm. Two sterile samples with size of 7–9 mm were implanted to parietal bones projection. Two similar samples were implanted into upper hip bones projection (Fig. 2).

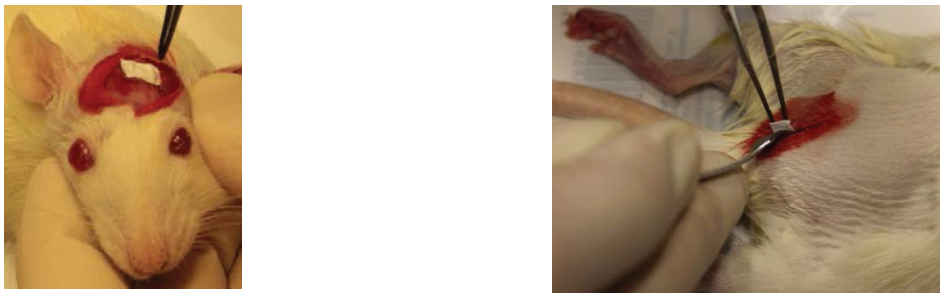

(a) (b)

FIGURE 2. Sample implantation on: (a) calvarial and (b) upper hip bones of rats

Before the implantation, subperiostal access to parietal and inner surface of upper hip bones was achieved with scarification of the cortical plate with raspatory. The implant was placed on scarified bone surface and fixed with muscle tissue.

After the samples implantation, the implantation cites were stitched with 4.0 suture and treated with septicide. Physical activity of the rats recovered in 15–19 min after awakening. The follow-up period was from 15 to 90 days. In case of purulence or sutures eruption, the animal was excluded from the experiment. The rats were weighted each 7 days.

Material Withdrawal

Four animals from each group were sacrificed after 15, 30, 60 and 90 days of experiment by narcosis (with Zoletil toxic doze of 35–40 mg/kg). Then, the tissue samples were prepared for morphological studies. For that purpose, calvarial and upper hip bones with implanted samples and covering muscle tissue were resected.

The tissue samples were fixed in 10% formalin for not less than 1 day. The bone tissue samples were decalcified in mixture of formic acid and 10% formalin with proportion of 1:4. Decalcification time was from several hours to 5–7 days. After that, the tissue was dehydrated and soaked in paraffin using Leica ASP-300S tissue processor. The sample was fixed in hystological cassetes. The slices 5–7 μm thick were prepared using Leica RM 2255 microtome, placed on object plates and stained with hematoxylin and eosin in Thermo Gemini AS stainer. Microscopy studies were carried out using "Zeiss Axio Scope" optical microscope at ×100 and ×200 magnifications.

Examination of 3D Implant Ability to Substitute the Bone Defects

The aim of following experiment was in one-step substitution of long bone circumferential defect with formation of bone inside, as well as on the surface of the implant.

To provide penetration of blood capillaries from the surrounding soft tissues and regeneration of intraosseous blood flow, the implant was fabricated as highly porous cylinder with the following dimensions: 40 mm high, 14 mm in diameter, 2 mm of wall thickness, depth of bone fitment bore of 10 mm.

The implant is presented as a porous cylinder with 300–500 μm open-ended inner pores crossing 1.0–1.5 mm cells. Such construction of the implant restores bone blood supply in periost, intramedullary blood flow and bone marrow, resulting in strong implant osteointegration.

Shin bone defect was simulated by resection of part of the diaphysis of dog shin bone 20 mm high, 15–18% of the bone length.

Taking into account the low strength of bioresorbable implant, primal osteosynthesis was carried out by Ilizarov frame for fixation of the implant. Then, tibial crest was exposed to longitudinal section with length of 40–50 mm and diaphysis was accessed by replacement of muscles and cortex. 20 mm section of the diaphysis was subperiosteal resected with vibrating saw. The implant was placed on adjacent ends of bones and cortex, soft tissues and skin were sutured.

RESULTS AND DISCUSSION

Osteointegration Properties of Bioresorbable Materials

Good implant fixation to surrounding muscle tissues (starting from 15 days of experiment) and cortex (starting from 60 days) was observed in all groups due to connective tissue invasion. The connective tissue membrane was transient and smooth.

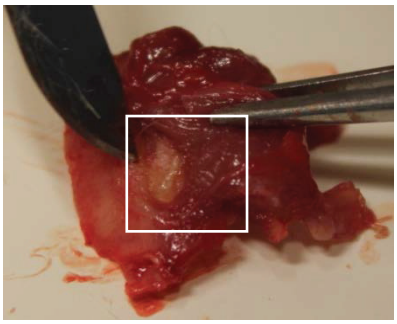
(a)
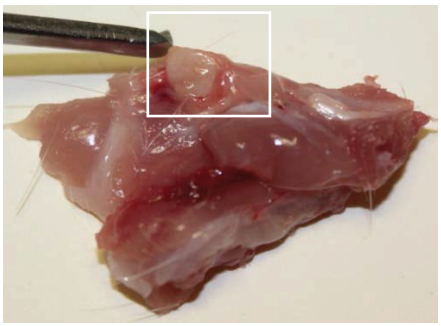
(b)

FIGURE 3. Withdrawal of Group 2 implant sample after 15 days: (a) upper hip and (b) calvarial bone

In 30 days of experiment, microvascular web was formed around the implant. Up to 15 days the implant was visualisable in surrounding muscle tissues as a white object (Fig. 3).

Thus, microscopic differences among the studied groups of implants withdrawn in different times were not found. Good integration of the implants into surrounding tissues, increasing biodegradation (from 15 to 90 days) and absence of visual signs of inflammation were noted.

Microscopy characterization of the implantation cites in different observation time (15, 30, 60 and 90 days) was conducted. The most interesting results were obtained in 90 days of experiment. In the first group, 70–90% resorption of the material was observed with the tendency to reduction of the number of giant cells and increase in fibroblasts. Slight osteogenesis in the areas contacting with bone was found (Fig. 4).

In the same period, in the second group irregular material resorption (50–100%) was observed. Remained giant cells-containing infiltrate demonstrated reduction in the number of giant cells and increase of fibroblasts. Significant osteogenesis was observed in all cases (Fig. 5).

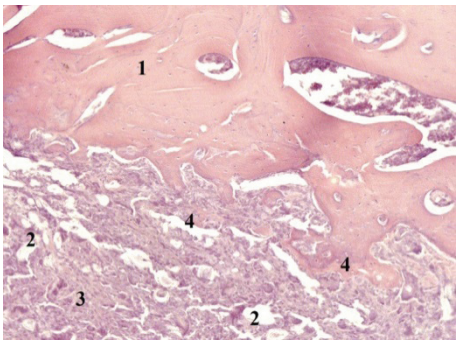

(a)
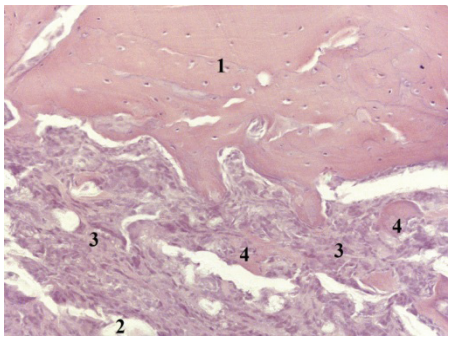

(b)

FIGURE 4. Group 1 after 90 days of implantation: *1*—bone tissue with signs of scarification, *2*—remained part of the implant, *3*—inflammatory infiltrate with multinucleate giant cells, *4*—formed bone rods. (a) ×100 magnification; (b) ×200 magnification

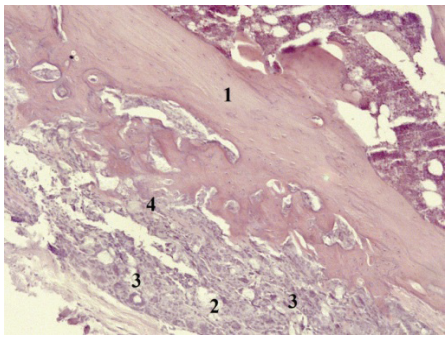

(a)
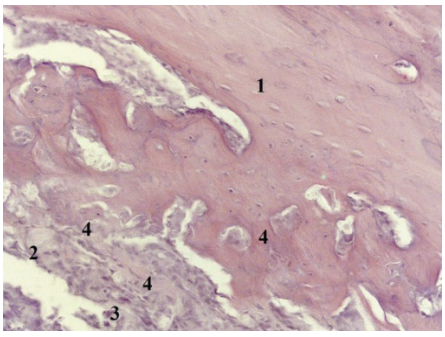

(b)

FIGURE 5. Group 2 after 90 days of implantation: *1*—bone tissue with signs of scarification, *2*—remained part of the implant, *3*—inflammatory infiltrate containing giant cells, *4*—formed bone rods. (a) ×100 magnification, (b) ×200 magnification

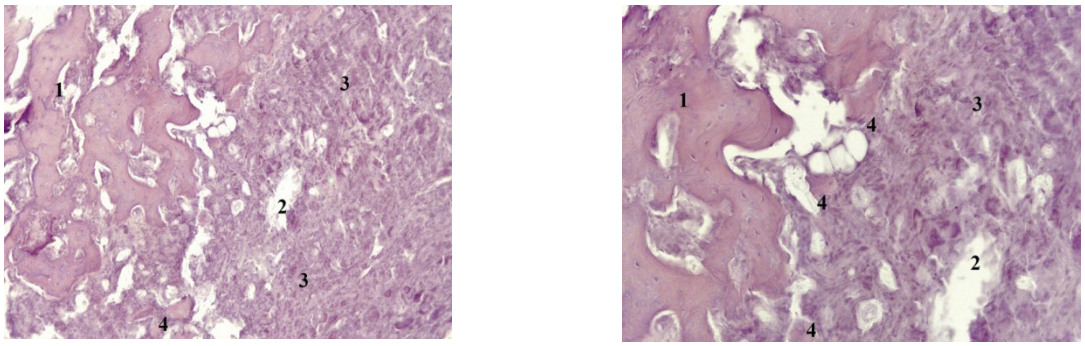

(a) (b)

FIGURE 6. Group 3 after 90 days of implantation: *1*—bone tissue with signs of scarification, *2*—remained part of the implant, *3*—inflammatory infiltrate containing giant cells, *4*—formed bone rods. (a) ×100 magnification, (b) ×200 magnification

At the end of experiment (90 days) irregular resorption (50–100%) of the material was observed in the third group. Remained giant cells-containing infiltrate demonstrated reduction of the number of giant cells and increase of fibroblasts. Significant osteogenesis was found only in 25% of cases, while in 75% it was slight and observed in areas contacted with bone (Fig. 6).

The conducted studies demonstrated that biodegradable implant made of PURASORB PL-38 poly(lactic acid) and hydrous dicalcium phosphate produced by laser ablation as filler induced more intensive osteogenesis.

Substitution of Bone Defects by Bioresorbable 3D Implants

The experiments on substitution of long bone circumferential defect (up to 18% of bone length) demonstrated that osteointegration of bioresorbable implant is equivalently intensive both from proximal and distal fragments (Fig. 7). A bone defect with a length of 20 mm was viewable in a post-operational X-ray image. The implant was transparent and produced no X-ray boundary (Fig. 7a).

X-ray boundary of bone graft appears after 14 days from the operation as a periosteal reaction around the implant shell (Fig. 7b). From the X-ray images it is obvious that bone graft X-ray boundary grows more intensively from proximal fragment (Fig. 7c). After two months of fixation, diastasis was nearly filled with bone graft and thin layer between proximal and distal fragments (Fig. 7d).

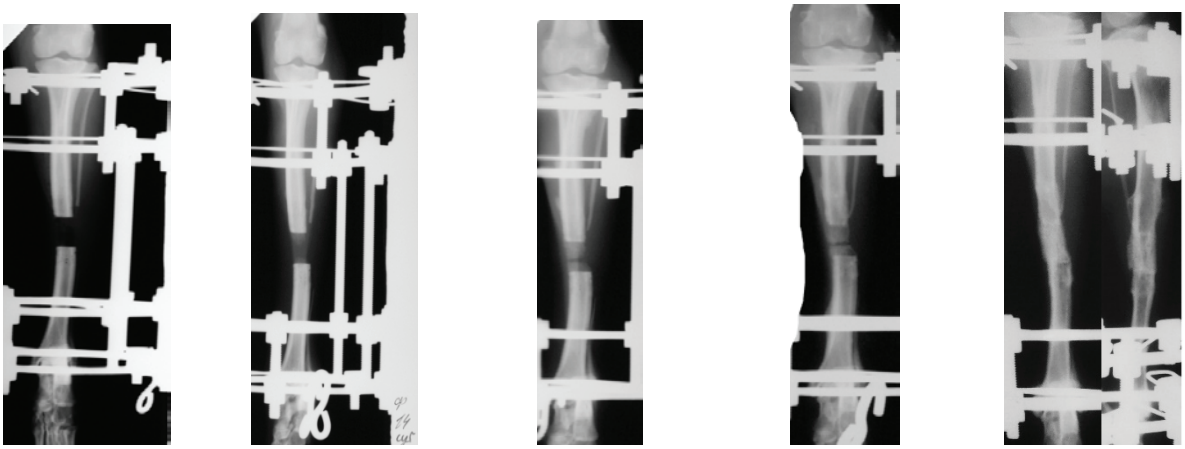

(a) (b) (c) (d) (e)

FIGURE 7. Radiographs of the lower leg of the experimental animal on the day of surgery (a); in the process of osteointegration of the bioresorbable implant after fixation (operation): (b) 14 days; (c) 35 days; (d) 2 months; (e) 4 months (in a straight line and lateral projections)

After 4 months of fixation (Fig. 7e), all parts of bone graft are connected into bone-implant complex, showing completed osteointegration.

During the post-operational period, high porosity of the implant supports circulation of biological fluids and allows them to penetrate into the implant. Also, it provides the ability of blood capillaries to grow into the implant.

CONCLUSION

The present article describes a promising method of implant fabrication combining computer tomogram technology and 3D-printing. The full process of personalized bone implant production is demonstrated. Moreover, the studies of novel composite materials made of bioresorbable polymer and various calcium phosphates in animal model show their effectiveness for formation of new bone tissue. Thus, the obtained data will be used for fabrication of personalized implants for bone defects substitution.

ACKNOWLEDGMENTS

This work was supported by Federal Medical Biological Agency (project Biopolymer-17).

REFERENCES

1. J. P. Shah and S. G. Patel, *Head and Neck Surgery and Oncology* (Mosby, 2013).
2. I. P. Janecka, Arch. Otolaryngol. Head Neck Surg. **126**, 396–401 (2000).
3. B. D. Ulery, L. S. Nair, and C. T. Laurencin, J. Polym. Sci. B. Polym. Phys. **49**, 832–864 (2011).
4. R. M. Rasal, A. V. Janorkar, and D. E Hirt, Prog. Polymer Sci. **35**, 338–356 (2010).
5. H. Tian, Z. Tang, X. Zhuang, X. Chen, and X. Jing, Prog. Polymer Sci. **37**, 237–280 (2012).
6. D. Rickert, *Polymeric Implant Materials for the Reconstruction of Tracheal and Pharyngeal Mucosal Defects in Head and Neck Surgery* (GMS Curr. Top Otorhinolaryngol. Head Neck Surg., 2009).
7. S. I. Goreninskii, N. N. Bogomolova, A. I. Malchikhina, A. S. Golovkin, E. N. Bolbasov, T. V. Safronova, V. I. Putlyaev, and S. I. Tverdokhlebov, BioNanoSci. **7**(1), 50–57 (2017).
8. S. I. Tverdokhlebov, E. N. Bolbasov, E. V. Shesterikov, L. V. Antonova, A. S. Golovkin, V. G. Matveeva, D. G. Petlin, and Y. G. Anissimov, Appl. Surf. Sci. **329**, 32–39 (2015).